EUROPEAN ORGANIZATION FOR NUCLEAR RESEARCH

CERN-PPE/97-106
6 August 1997

Neutral-Current Four-Fermion Production in e^+e^- Interactions at 130 GeV $\leq \sqrt{s} \leq$ 172 GeV

The L3 Collaboration

Abstract

A study of neutral-current four-fermion processes is performed, using data collected by the L3 detector at LEP during high-energy runs at centre-of-mass energies $130 - 136$, 161 and $170 - 172$ GeV, with integrated luminosities of 4.9, 10.7 and 10.1 pb^{-1}, respectively. The total cross sections for the final states $\ell\ell\ell'\ell'$ and $\ell\ell$qq (ℓ, ℓ' = e, μ or τ) are measured and found to be in agreement with the Standard Model prediction.

Submitted to *Phys. Lett. B*

Introduction

An observation of four-fermion events [1] from e^+e^- interactions above the expectations from the Standard Model would signal the existence of new physics. The four-fermion final states can arise from several production mechanisms, each giving a contribution to the cross section in a specific configuration of the final-particle phase space. In Fig. 1, all possible classes of neutral-current four-fermion production diagrams are shown. We will concentrate on the case where the outgoing fermions make at least a 5^0 angle with respect to the beam axis, in this way reducing the contribution from the multiperipheral diagrams. In this latter case, two quasi-real photons are exchanged in the t-channel giving rise to forward electrons/positrons plus a fermion pair with a non-resonant structure (the so-called "two-photon" process). This class of processes does not contribute to final states via Z exchange, where the main contributions come from the bremsstrahlung, conversion and annihilation diagrams. If an e^+e^- pair is present in the final state, the bremsstrahlung diagram is dominant, otherwise the conversion diagram contributes the most, mainly with an initial-state radiative photon and a Z boson on mass shell. This is in contrast to the situation at LEP1, where the annihilation mechanism dominates. Important characteristics of the four-fermion events are the energy and angular distributions of the outgoing fermions. If an e^+e^- pair is present in the final state, due to the multiperipheral or bremsstrahlung diagrams, the electrons tend to have nearly the beam energy and to be emitted along the beam direction. The other fermions in the event have preferentially lower energies, but still are predominantly generated in the forward direction. If no e^+e^- pair is present in the final state, the outgoing fermions have a flat energy distribution up to the beam energy and a forward angular distribution.

This letter analyses the final states produced at LEP2 by neutral-gauge-boson exchange, i.e. a γ or Z. These final states have already been observed at the Z resonance [2]. They can be classified as either $\ell\ell\ell'\ell'$ or $\ell\ell$qq events, where ℓ, $\ell' = $ e, μ or τ.

Data and Monte Carlo Samples

The data were collected by the L3 detector [3] at LEP in 1995 and 1996. The data sample corresponds to integrated luminosities of 4.9 pb^{-1}, 10.7 pb^{-1} and 10.1 pb^{-1} at $\sqrt{s} = 130.3 - 136.3$ GeV, 161.3 GeV and $170.3 - 172.3$ GeV, respectively.

To determine the efficiency of our selection criteria, the EXCALIBUR [4] Monte Carlo is used to simulate the four-fermion events. These events are generated requiring a minimum momentum for the outgoing fermions of 1 GeV, a minimum invariant mass for each combination of two fermions of 1 GeV and an angle of at least 5^0 for the outgoing fermions with respect to the beam axis, in this way reducing the contribution from the multiperipheral diagrams. Possible background comes from fermion-pair production and charged-current four-fermion events. For the fermion-pair production, radiative Bhabha events are generated using BHAGENE 3 [5] and radiative di-muon and di-tau samples using KORALZ 4.02 [6]. The hadronic background events are generated with PYTHIA 5.72 [7]. For the background coming from the charged-current four-fermion processes, i.e. where the W boson takes part in the process, KORALW 1.21 [8] and PYTHIA 5.718 [7] are used to simulate the reactions $e^+e^- \to$ WW and $e^+e^- \to$ Weν, respectively.

The L3 detector response is simulated using the GEANT 3.15 program [9], which takes into account the effects of energy loss, multiple scattering and showering in the detector. The GHEISHA program [10] is used to simulate hadronic interactions in the detector.

Four-fermion event selection

Two different event selections are developed, one for the low-multiplicity ($\ell\ell\ell'\ell'$) and another for the high-multiplicity ($\ell\ell$qq) topologies. The selected criteria for each are described below.

Lepton identification

Electrons

Electrons are identified as energy depositions in the electromagnetic calorimeter which are consistent with electromagnetic showers. If the calorimetric cluster is within $|\cos\theta| < 0.95$, a charged track from the central tracking chamber is required to be associated with it. The track must have a momentum greater than 0.5 GeV and a distance of closest approach to the interaction vertex in the plane perpendicular to the beam direction of less than 10 mm. The same track requirements are also used for the identification of the other leptons. The cluster is selected requiring $E_{\rm E} > 1$ GeV, where $E_{\rm E}$ is the energy deposited in the electromagnetic calorimeter. The corresponding deposition in the hadron calorimeter has to be consistent with the tail of an electromagnetic shower (i.e. $E_{\rm H}/E_{\rm E} < 0.2$ and $E_{\rm H} < 5$ GeV, where $E_{\rm H}$ is the energy in the hadronic calorimeter). Finally, the ratio of the energy in a 3x3 crystal matrix corrected for lateral leakage to the energy in a 5x5 crystal matrix centred around the center of gravity of the electromagnetic shower ($\Sigma 9/\Sigma 25$) is required to be greater than 0.93.

If the identified electrons are in hadronic events, as happens for the $\ell\ell$qq final states, the quality cuts are tightened and isolation cuts are applied to reject the background from hadronic semileptonic decays. We require that $\chi^2_{\rm em} < 4.5$, where the $\chi^2_{\rm em}$ is an estimator of the consistency of the shower being electromagnetic, and $\Sigma 9/\Sigma 25$ must be larger than 0.975. Moreover, the difference in the azimuthal angle between the electromagnetic cluster and the charged track must be less than 10 mrad, and there must not be more than one track in a cone with a 20^0 half-opening-angle around the electron.

Muons

Muons are identified as tracks in the muon chambers pointing to the interaction point. The calorimetric clusters and the tracks in the central chambers which are matched within 100 mrad in the azimuthal and polar angles are associated with those muons. Isolation criteria are applied to the identified muons if they are in hadronic events: the calorimetric energy in the region between cones of 5^0 and 10^0 half-opening-angles around the muon direction must be less than 5 GeV. The number of tracks in the central tracking chamber in a cone of 20^0 half-opening-angle around the muon direction has to be less than two. Finally, at most one calorimetric cluster is allowed in the angular region between 5^0 and 20^0 around the muon direction.

Taus

The hadronically-decaying taus are identified as one, two or three tracks with calorimetric energy greater than 2 GeV. Candidates with two tracks associated to the tau are kept to account for the finite double-track resolution of the central tracking chamber. The tau energy is defined as the energy of the clusters within a 10^0 angle around the tau-jet direction, which is computed as the sum of the momentum vectors of the calorimetric clusters. In order to separate the hadronic-tau candidates from other hadronic jets, the following restrictions are made: not more than one track and five calorimetric clusters in the region $10^0 < \alpha < 30^0$ are allowed, where

α is the half-opening-angle of a cone around the tau direction, and the ratio of the energies deposited in $10^0 < \alpha < 30^0$ and $\alpha < 10^0$ must be below 0.5. The leptonically-decaying taus are identified as either electrons or muons, as previously described.

The low-multiplicity event selection

To reject high-multiplicity events, we demand fewer than 10 charged tracks and fewer than 15 calorimetric clusters in the event. The visible energy is required to be larger than $0.2 \cdot \sqrt{s}$. At least three leptons are required in the event if there is a calorimetric deposition in the low-polar-angle detector, the forward lead-scintillator calorimeter (ALR). Otherwise, at least four leptons are required. Two of the selected leptons must have the same flavour. A minimum energy of 2 GeV for electrons and 3 GeV for muons and taus is required.

In Fig. 2, the comparison after all the cuts between the data and Monte Carlo is shown for the energy of all the leptons (excluding those in the ALR), the invariant mass of the pair of leptons of the same flavour with the highest invariant mass and the corresponding recoil mass. The recoil mass is defined as the missing mass against the chosen pair of leptons. In the first plot, there are at least three entries per event, depending on the number of selected leptons. The characteristics of the data events which survive the selection at the three centre-of-mass energies are listed in Table 1.

The high-multiplicity event selection

The $\ell\ell$qq events are characterized by hadronic jets and a pair of leptons isolated from the hadronic system. Only the configuration with a pair of isolated electrons or muons is investigated. No dedicated selection of $\tau\tau$qq events is performed, thus the surviving events come from the eeqq and $\mu\mu$qq selections. To select hadronic events, at least five charged tracks and 15 calorimetric clusters are required. The visible energy must be greater than $0.5 \cdot \sqrt{s}$ and, finally, a pair of electrons or muons, or an electron and a calorimetric deposition in the ALR is required. The energy of each lepton is required to exceed 3 GeV. The selected electrons and muons have to satisfy the isolation cuts and the tighter set of quality cuts since they are in a hadronic environment.

In Fig. 3, the distributions of the invariant mass of the two selected leptons and their recoil mass are shown for the data and Monte Carlo, after the cuts. All data events which survive the selection contain two identified electrons; no event with two muons is found. The data events which pass the selection at the three centre-of-mass energies are listed in Table 1, where the invariant mass and the recoil mass of the two electrons are presented.

Efficiencies and systematic errors

The selection efficiency for signal events is evaluated using Monte Carlo simulation. The efficiencies of the low-multiplicity and high-multiplicity event selections are given in Table 2 with the corresponding systematic errors from the Monte Carlo statistics only. The efficiencies are calculated for events in which all four-fermions have an angle of at least 5^0 with respect to the beam axis. From Table 2, it can be seen that the cross feeding between channels is very small. The main sources of systematic errors are the detector uncertainties and inefficiencies, which include:

a) uncertainty on the energy intercalibration constants;
b) uncertainty on the global energy scale;
c) uncertainty on the tracking inefficiency;

and the Monte Carlo statistics. To estimate effect a), each energy calibration constant was varied independently according to a normal distribution with a standard deviation of 5%, as explained in detail in reference [11]. To estimate effect b), the total energy was shifted by $\pm 3\%$ and, finally, to take into account effect c), 2%, of the tracks were randomly eliminated in the Monte Carlo events. The net effect of these errors due to the detector systematics on the signal efficiency is found to be at most 2%, which is usually less than the Monte Carlo statistical error.

The dominant error on the number of expected background events is also due to the Monte Carlo statistics, which gives a contribution of at least 10%. Moreover, an overall normalisation error, estimated to be 10%, due to the finite precision of the event generators is taken into account.

Results

The total number of events expected from the signal, the background and the number of events observed in the data after all the cuts are shown in Table 3, where the total error is also reported.

Due to the lack of statistics, the cross sections $\sigma_{\ell\ell\ell'\ell'}$ and $\sigma_{\ell\ell\mathrm{qq}}$ of the processes $\mathrm{e^+e^-} \to \ell\ell\ell'\ell'$ and $\mathrm{e^+e^-} \to \ell\ell\mathrm{qq}$ are determined simultaneously in a one-variable maximum-likelihood fit by fixing the ratio of the two cross sections to the Standard Model value. This corresponds to a determination of the total cross section $\sigma_{\mathrm{tot}} = \sigma_{\ell\ell\ell'\ell'} + \sigma_{\ell\ell\mathrm{qq}}$. The measurement of this total cross section is done independently for the three centre-of-mass energies. The total likelihood is given by the product of the Poisson probabilities, $P(N_i, \mu_i)$, for the low-multiplicity ($i = 1$) and high-multiplicity ($i = 2$) selections, where N_i is the number of selected events and μ_i the number of expected events:

$$\mu_i = \sum_{j=1,2} \epsilon_{ij}\sigma_j L_i + N_i^{\mathrm{bkgd}}.$$

Here, ϵ_{ij} is the efficiency of selection i to accept events from process j, where j=1 for the $\ell\ell\ell'\ell'$ channel and j=2 for the $\ell\ell\mathrm{qq}$ channel. Moreover, N_i^{bkgd} is the number of expected background events and L_i is the integrated luminosity for selection i. Finally, σ_j is the cross section for process j. The systematic error on the cross section is estimated as the RMS of the measured cross section obtained with a random variation of the signal efficiency and the number of expected background events, according to their total errors. The measured total cross sections are:

$$\begin{array}{lcrcrcrcl}
\sigma_{\mathrm{tot}} & = & 2.9\ ^{+\ 4.2}_{-\ 2.6} & (\mathrm{stat.}) & \pm\ 0.17 & (\mathrm{sys.})\ \mathrm{pb} & (5.2\ \mathrm{pb}) & \text{at } \sqrt{s} & = 133\ \mathrm{GeV} \\
\sigma_{\mathrm{tot}} & = & 3.2\ ^{+\ 2.7}_{-\ 1.8} & (\mathrm{stat.}) & \pm\ 0.06 & (\mathrm{sys.})\ \mathrm{pb} & (3.4\ \mathrm{pb}) & \text{at } \sqrt{s} & = 161\ \mathrm{GeV} \\
\sigma_{\mathrm{tot}} & = & 4.1\ ^{+\ 3.0}_{-\ 2.1} & (\mathrm{stat.}) & \pm\ 0.08 & (\mathrm{sys.})\ \mathrm{pb} & (3.2\ \mathrm{pb}) & \text{at } \sqrt{s} & = 172\ \mathrm{GeV}
\end{array}$$

The Standard Model values for the cross sections are given in parentheses.
Assuming the scaling of the cross sections with energy from the Standard Model, $\sigma_{\ell\ell\ell'\ell'}$ and $\sigma_{\ell\ell\mathrm{qq}}$ at any energy can be taken as unknown parameters to be measured independently. For instance at $\sqrt{s} = 161$ GeV:

$$\sigma^{161}_{\ell\ell\ell'\ell'} = 2.0\ ^{+}_{-}\ ^{1.2}_{0.9}\ \text{(stat.)} \pm 0.04\ \text{(sys.)}\ \text{pb}$$
$$\sigma^{161}_{\ell\ell\mathrm{qq}} = 1.3\ ^{+}_{-}\ ^{1.1}_{0.8}\ \text{(stat.)} \pm 0.03\ \text{(sys.)}\ \text{pb}$$

Finally, assuming both the scaling with energy and the ratio of the cross sections $\sigma_{\ell\ell\ell'\ell'}$ and $\sigma_{\ell\ell\mathrm{qq}}$ from the Standard Model, only one parameter is left free in the fit. Chosing the total cross section at $\sqrt{s} = 161$ GeV as free parameter, we measure:

$$\sigma^{161}_{\mathrm{tot}} = 3.3\ ^{+}_{-}\ ^{1.6}_{1.3}\ \text{(stat.)} \pm 0.05\ \text{(sys.)}\ \text{pb}$$

The results agree with the Standard Model predictions and there is no indication of any new physics.

Acknowledgments

We wish to express our gratitude to the CERN accelerator divisions for the excellent performance of the LEP machine. We acknowledge the contributions of all the engineers and technicians who have participated in the construction and maintenance of this experiment.

References

[1] "Physics at LEP2", Eds. G.Altarelli, T.Sjöstrand and F.Zwirner, CERN 96-01 (1996).

[2] L3 Collaboration, A. Adam *et al.*, Phys. Lett. **B 321** (1994) 283.

[3] L3 Collaboration, B. Adeva *et al.*, Nucl. Instr. Meth. **A 289** (1990) 35; J. A. Bakken *et al.*, Nucl. Instr. Meth. **A 275** (1989) 81; O. Adriani *et al.*, Nucl. Instr. Meth. **A 302** (1991) 53; B. Adeva *et al.*, Nucl. Instr. Meth. **A 323** (1992) 109; K. Deiters *et al.*, Nucl. Instr. Meth. **A 323** (1992) 162; M. Chemarin *et al.*, Nucl. Instr. Meth. **A 349** (1994) 345; B. Acciari *et al.*, Nucl. Instr. Meth. **A 351** (1994) 300; G. Basti *et al.*, Nucl. Instr. Meth. **A 374** (1996) 293; A. Adam *et al.*, Nucl. Instr. Meth. **A 383** (1996) 342.

[4] F. A. Berends, R. Kleiss and R. Pittau, Nucl. Phys. **B 424** (1994) 308; Nucl. Phys. **B 426** (1994) 344; Nucl. Phys. (Proc. Suppl.) **B 37** (1994) 163; Phys. Lett. **B 335** (1994) 490; R. Kleiss and R. Pittau, Comp. Phys. Comm. **83** (1994) 14.

[5] J. H. Field, Phys. Lett. **B 323** (1994) 432; J. H. Field and T. Riemann, Comp. Phys. Comm. **94** (1996) 53.

[6] S. Jadach, B. F. L. Ward and Z. Wąs, Comp. Phys. Comm. **79** (1994) 503.

[7] T. Sjöstrand, CERN-TH/7112/93 (1993), revised August 1995; T. Sjöstrand, Comp. Phys. Comm. **82** (1994) 74; T. Sjöstrand, CERN-TH 7112/93 (1993, revised August 1994).

[8] M. Skrzypek *et al.*, Comp. Phys. Comm. **94** (1996) 216; M. Skrzypek *et al.*, Phys. Lett. **B 372** (1996) 289.

[9] R. Brun *et al.*, preprint CERN DD/EE/84-1 (Revised 1987).

[10] H. Fesefeldt, RWTH Aachen Report PITHA 85/02 (1985).

[11] L3 Collaboration, M. Acciarri *et al.*, Phys. Lett. **B 385** (1996) 454.

The L3 Collaboration:

M.Acciarri,[29] O.Adriani,[18] M.Aguilar-Benitez,[28] S.Ahlen,[12] J.Alcaraz,[28] G.Alemanni,[24] J.Allaby,[19] A.Aloisio,[31] G.Alverson,[13] M.G.Alviggi,[31] G.Ambrosi,[21] H.Anderhub,[51] V.P.Andreev,[7,40] T.Angelescu,[14] F.Anselmo,[10] A.Arefiev,[30] T.Azemoon,[3] T.Aziz,[11] P.Bagnaia,[39] L.Baksay,[46] S.Banerjee,[11] Sw.Banerjee,[11] K.Banicz,[48] A.Barczyk,[51,49] R.Barillère,[19] L.Barone,[39] P.Bartalini,[36] A.Baschirotto,[29] M.Basile,[10] R.Battiston,[36] A.Bay,[24] F.Becattini,[18] U.Becker,[17] F.Behner,[51] J.Berdugo,[28] P.Berges,[17] B.Bertucci,[36] B.L.Betev,[51] S.Bhattacharya,[11] M.Biasini,[19] A.Biland,[51] G.M.Bilei,[36] J.J.Blaising,[4] S.C.Blyth,[37] G.J.Bobbink,[2] R.Bock,[1] A.Böhm,[1] L.Boldizsar,[15] B.Borgia,[39] D.Bourilkov,[51] M.Bourquin,[21] S.Braccini,[21] J.G.Branson,[42] V.Brigljevic,[51] I.C.Brock,[37] A.Buffini,[18] A.Buijs,[47] J.D.Burger,[17] W.J.Burger,[21] J.Busenitz,[46] A.Button,[3] X.D.Cai,[17] M.Campanelli,[51] M.Capell,[17] G.Cara Romeo,[10] G.Carlino,[31] A.M.Cartacci,[18] J.Casaus,[28] G.Castellini,[18] F.Cavallari,[39] N.Cavallo,[31] C.Cecchi,[21] M.Cerrada,[28] F.Cesaroni,[25] M.Chamizo,[28] Y.H.Chang,[53] U.K.Chaturvedi,[20] S.V.Chekanov,[33] M.Chemarin,[27] A.Chen,[53] G.Chen,[8] G.M.Chen,[8] H.F.Chen,[22] H.S.Chen,[8] X.Chereau,[4] G.Chiefari,[31] C.Y.Chien,[5] L.Cifarelli,[41] F.Cindolo,[10] C.Civinini,[18] I.Clare,[17] R.Clare,[17] H.O.Cohn,[34] G.Coignet,[4] A.P.Colijn,[2] N.Colino,[28] V.Commichau,[1] S.Costantini,[9] F.Cotorobai,[14] B.de la Cruz,[28] A.Csilling,[15] T.S.Dai,[17] R.D'Alessandro,[18] R.de Asmundis,[31] A.Degré,[4] K.Deiters,[49] D.della Volpe,[31] P.Denes,[38] F.DeNotaristefani,[39] D.DiBitonto,[46] M.Diemoz,[39] D.van Dierendonck,[2] F.Di Lodovico,[51] C.Dionisi,[39] M.Dittmar,[51] A.Dominguez,[42] A.Doria,[31] M.T.Dova,[20,♯] D.Duchesneau,[4] P.Duinker,[2] I.Duran,[43] S.Dutta,[11] S.Easo,[36] Yu.Efremenko,[34] H.El Mamouni,[27] A.Engler,[37] F.J.Eppling,[17] F.C.Erné,[2] J.P.Ernenwein,[27] P.Extermann,[21] M.Fabre,[49] R.Faccini,[39] S.Falciano,[39] A.Favara,[18] J.Fay,[27] O.Fedin,[40] M.Felcini,[51] B.Fenyi,[46] T.Ferguson,[37] F.Ferroni,[39] H.Fesefeldt,[1] E.Fiandrini,[36] J.H.Field,[21] F.Filthaut,[37] P.H.Fisher,[17] I.Fisk,[42] G.Forconi,[17] L.Fredj,[21] K.Freudenreich,[51] C.Furetta,[29] Yu.Galaktionov,[30,17] S.N.Ganguli,[11] P.Garcia-Abia,[50] S.S.Gau,[13] S.Gentile,[39] N.Gheordanescu,[14] S.Giagu,[39] S.Goldfarb,[24] J.Goldstein,[12] Z.F.Gong,[22] A.Gougas,[5] G.Gratta,[35] M.W.Gruenewald,[9] V.K.Gupta,[38] A.Gurtu,[11] L.J.Gutay,[48] B.Hartmann,[1] A.Hasan,[32] D.Hatzifotiadou,[10] T.Hebbeker,[9] A.Hervé,[19] W.C.van Hoek,[33] H.Hofer,[51] S.J.Hong,[45] H.Hoorani,[37] S.R.Hou,[53] G.Hu,[5] V.Innocente,[19] K.Jenkes,[1] B.N.Jin,[8] L.W.Jones,[3] P.de Jong,[19] I.Josa-Mutuberria,[28] A.Kasser,[24] R.A.Khan,[20] D.Kamrad,[50] Yu.Kamyshkov,[34] J.S.Kapustinsky,[26] Y.Karyotakis,[4] M.Kaur,[20,◇] M.N.Kienzle-Focacci,[21] D.Kim,[39] D.H.Kim,[45] J.K.Kim,[45] S.C.Kim,[45] Y.G.Kim,[45] W.W.Kinnison,[26] A.Kirkby,[35] D.Kirkby,[35] J.Kirkby,[19] D.Kiss,[15] W.Kittel,[33] A.Klimentov,[17,30] A.C.König,[33] A.Kopp,[50] I.Korolko,[30] V.Koutsenko,[17,30] R.W.Kraemer,[37] W.Krenz,[1] A.Kunin,[17,30] P.Ladron de Guevara,[28] I.Laktineh,[27] G.Landi,[18] C.Lapoint,[17] K.Lassila-Perini,[51] P.Laurikainen,[23] M.Lebeau,[19] A.Lebedev,[17] P.Lebrun,[27] P.Lecomte,[51] P.Lecoq,[19] P.Le Coultre,[51] H.J.Lee,[9] J.M.Le Goff,[19] R.Leiste,[50] E.Leonardi,[39] P.Levtchenko,[40] C.Li,[22] C.H.Lin,[53] W.T.Lin,[53] F.L.Linde,[2,19] L.Lista,[31] Z.A.Liu,[8] W.Lohmann,[50] E.Longo,[39] W.Lu,[35] Y.S.Lu,[8] K.Lübelsmeyer,[1] C.Luci,[39] D.Luckey,[17] L.Luminari,[39] W.Lustermann,[49] W.G.Ma,[22] M.Maity,[11] G.Majumder,[11] L.Malgeri,[39] A.Malinin,[30] C.Maña,[28] D.Mangeol,[33] S.Mangla,[11] P.Marchesini,[51] A.Marin,[12] J.P.Martin,[27] F.Marzano,[39] G.G.G.Massaro,[2] D.McNally,[19] R.R.McNeil,[7] S.Mele,[31] L.Merola,[31] M.Meschini,[18] W.J.Metzger,[33] M.von der Mey,[1] Y.Mi,[24] A.Mihul,[14] A.J.W.van Mil,[33] H.Milcent,[19] G.Mirabelli,[39] J.Mnich,[19] P.Molnar,[9] B.Monteleoni,[18] R.Moore,[3] S.Morganti,[39] T.Moulik,[11] R.Mount,[35] S.Müller,[1] F.Muheim,[21] A.J.M.Muijs,[2] S.Nahn,[17] M.Napolitano,[31] F.Nessi-Tedaldi,[51] H.Newman,[35] T.Niessen,[1] A.Nippe,[1] A.Nisati,[39] H.Nowak,[50] Y.D.Oh,[45] H.Opitz,[1] G.Organtini,[39] R.Ostonen,[23] C.Palomares,[28] D.Pandoulas,[1] S.Paoletti,[39] P.Paolucci,[31] H.K.Park,[37] I.H.Park,[45] G.Pascale,[39] G.Passaleva,[19] S.Patricelli,[31] T.Paul,[13] M.Pauluzzi,[36] C.Paus,[19] F.Pauss,[51] D.Peach,[19] Y.J.Pei,[1] S.Pensotti,[29] D.Perret-Gallix,[4] B.Petersen,[33] S.Petrak,[9] A.Pevsner,[5] D.Piccolo,[31] M.Pieri,[18] P.A.Piroué,[38] E.Pistolesi,[29] V.Plyaskin,[30] M.Pohl,[51] V.Pojidaev,[30,18] H.Postema,[17] N.Produit,[21] D.Prokofiev,[40] G.Rahal-Callot,[51] N.Raja,[11] P.G.Rancoita,[29] M.Rattaggi,[29] G.Raven,[42] P.Razis,[32] K.Read,[34] D.Ren,[51] M.Rescigno,[39] S.Reucroft,[13] T.van Rhee,[47] S.Riemann,[50] K.Riles,[3] A.Robohm,[51] J.Rodin,[17] B.P.Roe,[3] L.Romero,[28] S.Rosier-Lees,[4] Ph.Rosselet,[24] W.van Rossum,[47] S.Roth,[1] J.A.Rubio,[19] D.Ruschmeier,[9] H.Rykaczewski,[51] J.Salicio,[19] E.Sanchez,[28] M.P.Sanders,[33] M.E.Sarakinos,[23] S.Sarkar,[11] M.Sassowsky,[1] C.Schäfer,[1] V.Schegelsky,[40] S.Schmidt-Kaerst,[1] D.Schmitz,[1] P.Schmitz,[1] N.Scholz,[51] H.Schopper,[52] D.J.Schotanus,[33] J.Schwenke,[1] G.Schwering,[1] C.Sciacca,[31] D.Sciarrino,[21] L.Servoli,[36] S.Shevchenko,[35] N.Shivarov,[44] V.Shoutko,[30] J.Shukla,[26] E.Shumilov,[30] A.Shvorob,[35] T.Siedenburg,[1] D.Son,[45] A.Sopczak,[50] B.Smith,[17] P.Spillantini,[18] M.Steuer,[17] D.P.Stickland,[38] A.Stone,[7] H.Stone,[38] B.Stoyanov,[44] A.Straessner,[1] K.Strauch,[16] K.Sudhakar,[11] G.Sultanov,[20] L.Z.Sun,[22] G.F.Susinno,[21] H.Suter,[51] J.D.Swain,[20] X.W.Tang,[8] L.Tauscher,[6] L.Taylor,[13] Samuel C.C.Ting,[17] S.M.Ting,[17] M.Tonutti,[1] S.C.Tonwar,[11] J.Tóth,[15] C.Tully,[38] H.Tuchscherer,[46] K.L.Tung,[8] Y.Uchida,[17] J.Ulbricht,[51] U.Uwer,[19] E.Valente,[39] R.T.Van de Walle,[33] G.Vesztergombi,[15] I.Vetlitsky,[30] G.Viertel,[51] M.Vivargent,[4] R.Völkert,[50] H.Vogel,[37] H.Vogt,[50] I.Vorobiev,[19,30] A.A.Vorobyov,[40] A.Vorvolakos,[32] M.Wadhwa,[6] W.Wallraff,[1] J.C.Wang,[17] X.L.Wang,[22] Z.M.Wang,[22] A.Weber,[1] F.Wittgenstein,[19] S.X.Wu,[20] S.Wynhoff,[1] J.Xu,[12] Z.Z.Xu,[22] B.Z.Yang,[22] C.G.Yang,[8] X.Y.Yao,[8] J.B.Ye,[22] S.C.Yeh,[53] J.M.You,[37] An.Zalite,[40] Yu.Zalite,[40] P.Zemp,[51] Y.Zeng,[1] Z.Zhang,[8] Z.P.Zhang,[22] B.Zhou,[12] G.Y.Zhu,[8] R.Y.Zhu,[35] A.Zichichi,[10,19,20] F.Ziegler.[50]

1 I. Physikalisches Institut, RWTH, D-52056 Aachen, FRG[§]
III. Physikalisches Institut, RWTH, D-52056 Aachen, FRG[§]
2 National Institute for High Energy Physics, NIKHEF, and University of Amsterdam, NL-1009 DB Amsterdam, The Netherlands
3 University of Michigan, Ann Arbor, MI 48109, USA
4 Laboratoire d'Annecy-le-Vieux de Physique des Particules, LAPP,IN2P3-CNRS, BP 110, F-74941 Annecy-le-Vieux CEDEX, France
5 Johns Hopkins University, Baltimore, MD 21218, USA
6 Institute of Physics, University of Basel, CH-4056 Basel, Switzerland
7 Louisiana State University, Baton Rouge, LA 70803, USA
8 Institute of High Energy Physics, IHEP, 100039 Beijing, China[△]
9 Humboldt University, D-10099 Berlin, FRG[§]
10 University of Bologna and INFN-Sezione di Bologna, I-40126 Bologna, Italy
11 Tata Institute of Fundamental Research, Bombay 400 005, India
12 Boston University, Boston, MA 02215, USA
13 Northeastern University, Boston, MA 02115, USA
14 Institute of Atomic Physics and University of Bucharest, R-76900 Bucharest, Romania
15 Central Research Institute for Physics of the Hungarian Academy of Sciences, H-1525 Budapest 114, Hungary[‡]
16 Harvard University, Cambridge, MA 02139, USA
17 Massachusetts Institute of Technology, Cambridge, MA 02139, USA
18 INFN Sezione di Firenze and University of Florence, I-50125 Florence, Italy
19 European Laboratory for Particle Physics, CERN, CH-1211 Geneva 23, Switzerland
20 World Laboratory, FBLJA Project, CH-1211 Geneva 23, Switzerland
21 University of Geneva, CH-1211 Geneva 4, Switzerland
22 Chinese University of Science and Technology, USTC, Hefei, Anhui 230 029, China[△]
23 SEFT, Research Institute for High Energy Physics, P.O. Box 9, SF-00014 Helsinki, Finland
24 University of Lausanne, CH-1015 Lausanne, Switzerland
25 INFN-Sezione di Lecce and Universitá Degli Studi di Lecce, I-73100 Lecce, Italy
26 Los Alamos National Laboratory, Los Alamos, NM 87544, USA
27 Institut de Physique Nucléaire de Lyon, IN2P3-CNRS,Université Claude Bernard, F-69622 Villeurbanne, France
28 Centro de Investigaciones Energeticas, Medioambientales y Tecnologicas, CIEMAT, E-28040 Madrid, Spain[♭]
29 INFN-Sezione di Milano, I-20133 Milan, Italy
30 Institute of Theoretical and Experimental Physics, ITEP, Moscow, Russia
31 INFN-Sezione di Napoli and University of Naples, I-80125 Naples, Italy
32 Department of Natural Sciences, University of Cyprus, Nicosia, Cyprus
33 University of Nijmegen and NIKHEF, NL-6525 ED Nijmegen, The Netherlands
34 Oak Ridge National Laboratory, Oak Ridge, TN 37831, USA
35 California Institute of Technology, Pasadena, CA 91125, USA
36 INFN-Sezione di Perugia and Universitá Degli Studi di Perugia, I-06100 Perugia, Italy
37 Carnegie Mellon University, Pittsburgh, PA 15213, USA
38 Princeton University, Princeton, NJ 08544, USA
39 INFN-Sezione di Roma and University of Rome, "La Sapienza", I-00185 Rome, Italy
40 Nuclear Physics Institute, St. Petersburg, Russia
41 University and INFN, Salerno, I-84100 Salerno, Italy
42 University of California, San Diego, CA 92093, USA
43 Dept. de Fisica de Particulas Elementales, Univ. de Santiago, E-15706 Santiago de Compostela, Spain
44 Bulgarian Academy of Sciences, Central Lab. of Mechatronics and Instrumentation, BU-1113 Sofia, Bulgaria
45 Center for High Energy Physics, Korea Adv. Inst. of Sciences and Technology, 305-701 Taejon, Republic of Korea
46 University of Alabama, Tuscaloosa, AL 35486, USA
47 Utrecht University and NIKHEF, NL-3584 CB Utrecht, The Netherlands
48 Purdue University, West Lafayette, IN 47907, USA
49 Paul Scherrer Institut, PSI, CH-5232 Villigen, Switzerland
50 DESY-Institut für Hochenergiephysik, D-15738 Zeuthen, FRG
51 Eidgenössische Technische Hochschule, ETH Zürich, CH-8093 Zürich, Switzerland
52 University of Hamburg, D-22761 Hamburg, FRG
53 High Energy Physics Group, Taiwan, China

§ Supported by the German Bundesministerium für Bildung, Wissenschaft, Forschung und Technologie
‡ Supported by the Hungarian OTKA fund under contract numbers T14459 and T24011.
♭ Supported also by the Comisión Interministerial de Ciencia y Tecnología
♯ Also supported by CONICET and Universidad Nacional de La Plata, CC 67, 1900 La Plata, Argentina
♢ Also supported by Panjab University, Chandigarh-160014, India
△ Supported by the National Natural Science Foundation of China.

Low-multiplicity selection			
$\sqrt{s}$ (GeV)	Final State	$M_{\ell\ell}^{\max}$(GeV)	$M_{\rm rec}$(GeV)
130.3	ee$\mu\mu$	85.7 ± 0.8	39 ± 3
161.3	$\mu\mu$ee	10.1 ± 0.2	108 ± 2
161.3	$\mu\mu$ee	84.7 ± 2.7	35 ± 16
172.3	eeee	161.9 ± 1.3	-
172.3	eeee	66.8 ± 0.6	23 ± 7
High-multiplicity selection			
$\sqrt{s}$(GeV)	Final State	$M_{\ell\ell}$(GeV)	$M_{\rm rec}$(GeV)
136.3	eeqq	81 ± 10	49 ± 5
161.3	eeqq	78.1 ± 0.7	38 ± 4
172.3	eeqq	76.2 ± 0.7	39 ± 4
172.3	eeqq	145.1 ± 1.2	11 ± 24

Table 1: Candidate events from the low-multiplicity and high-multiplicity selections: the centre-of-mass energy, the observed final state, the lepton-pair invariant mass and the corresponding recoil mass are reported. For the low-multiplicity selection the lepton-pair used in the calculation is the one with the highest invariant mass, excluding leptons tagged by the ALR. This corresponds to the first lepton-pair reported in the second column. Negative squared invariant masses are not reported.

Signal efficiencies			
Selection	$\sqrt{s}$	$\ell\ell\ell'\ell'$ Channel	$\ell\ell$qq Channel
Low-multiplicity	$130 - 136$ GeV	$(8.1 \pm 0.3)\%$	$(0.06 \pm 0.02)\%$
	161 GeV	$(6.8 \pm 0.2)\%$	$(0.05 \pm 0.01)\%$
	$170 - 172$ GeV	$(7.7 \pm 0.2)\%$	$(0.08 \pm 0.02)\%$
High-multiplicity	$130 - 136$ GeV	$(0.32 \pm 0.06)\%$	$(8.5 \pm 0.3)\%$
	161 GeV	$(0.27 \pm 0.03)\%$	$(7.1 \pm 0.2)\%$
	$170 - 172$ GeV	$(0.25 \pm 0.03)\%$	$(7.7 \pm 0.2)\%$

Table 2: Low-multiplicity and high-multiplicity event selection efficiencies for the $\ell\ell\ell'\ell'$ and $\ell\ell$qq channels, with the corresponding Monte Carlo statistical error, for the three centre-of-mass energies.

Process	$\sqrt{s} = 130 - 136$ GeV	$\sqrt{s} = 161$ GeV	$\sqrt{s} = 170 - 172$ GeV
eeee	0.50 ± 0.02	0.66 ± 0.04	0.65 ± 0.04
ee$\mu\mu$	0.29 ± 0.02	0.38 ± 0.06	0.35 ± 0.05
ee$\tau\tau$	0.10 ± 0.01	0.14 ± 0.03	0.13 ± 0.03
$\mu\mu\mu\mu$	0.0250 ± 0.0008	0.029 ± 0.002	0.024 ± 0.002
$\mu\mu\tau\tau$	0.024 ± 0.001	0.029 ± 0.003	0.025 ± 0.002
$\tau\tau\tau\tau$	0.0034 ± 0.0004	0.0051 ± 0.0009	0.0034 ± 0.0006
$\ell\ell\ell'\ell'$	0.95 ± 0.03	1.23 ± 0.08	1.18 ± 0.07
eeqq	0.93 ± 0.03	1.16 ± 0.06	1.09 ± 0.06
$\mu\mu$qq	0.210 ± 0.004	0.27 ± 0.01	0.29 ± 0.01
$\tau\tau$qq	0.012 ± 0.001	0.014 ± 0.002	0.012 ± 0.002
$\ell\ell$qq	1.15 ± 0.03	1.45 ± 0.06	1.40 ± 0.06
Total Signal	2.10 ± 0.04	2.7 ± 0.1	2.56 ± 0.09
Background	0.8 ± 0.3	0.71 ± 0.09	0.8 ± 0.2
Data	2	3	4

Table 3: The number of expected four-fermion and background events, with their total errors, and the number of data events observed at the three centre-of-mass energies.

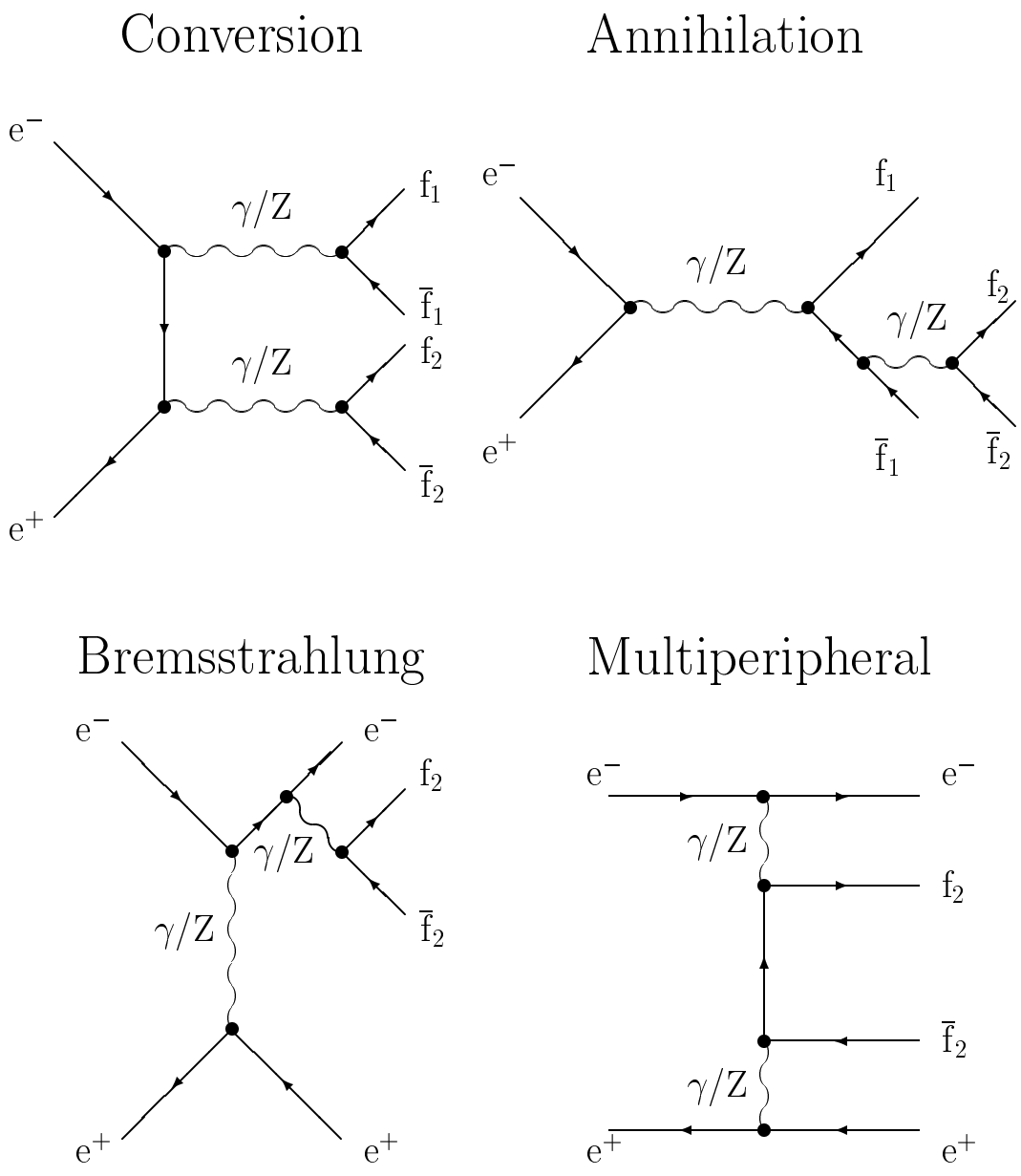

Figure 1: The lowest-order Feynman diagrams for the process $e^+e^- \to f_1\bar{f}_1f_2\bar{f}_2$.

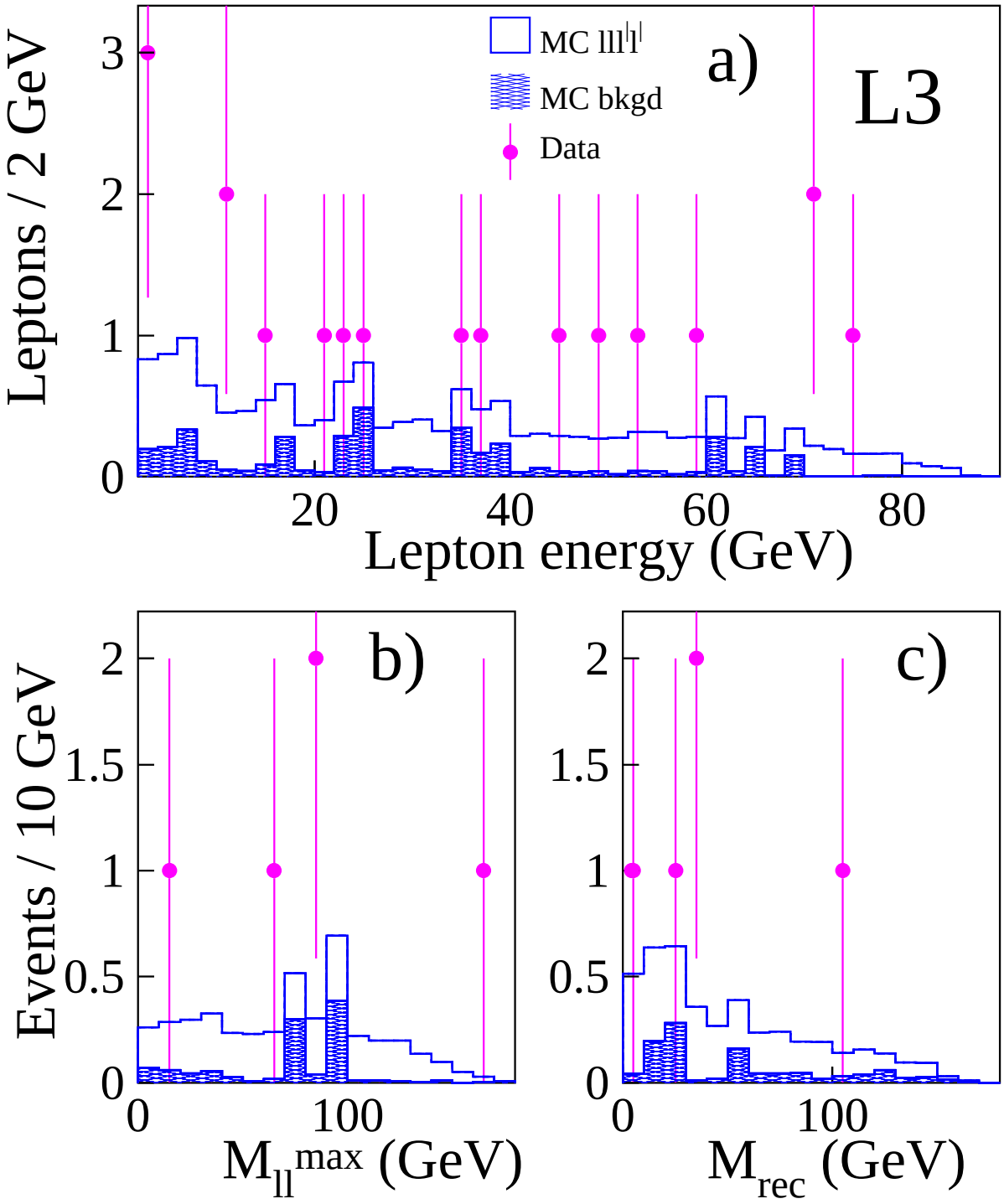

Figure 2: Distributions for the low-multiplicity selection ($\ell\ell\ell'\ell'$) of (a) the lepton energy, (b) the highest lepton-pair invariant mass per event for leptons of the same flavour and (c) the corresponding recoil mass. The open histograms are the Monte Carlo predicted four-fermion distributions, the hatched histograms are the Monte Carlo predicted background distributions and the points are the data events.

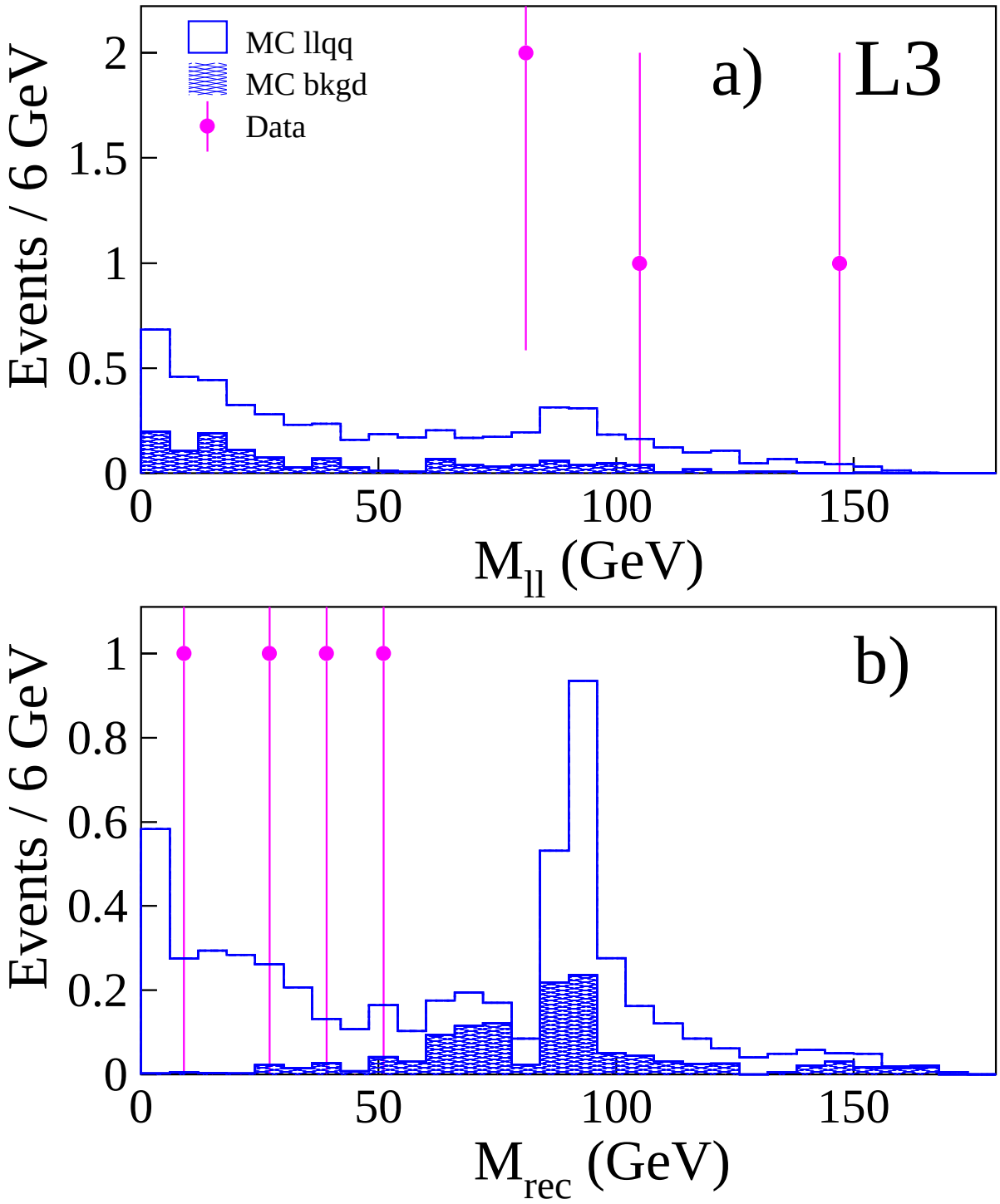

Figure 3: Distributions for the high-multiplicity selection ($\ell\ell$qq) of (a) the lepton-pair invariant mass and (b) the their recoil mass. The open histograms are the Monte Carlo predicted four-fermion distributions, the hatched histograms are the Monte Carlo predicted background distributions and the points are the data events.